Buenos Aires – 5 to 9 September 2016
Acoustics for the 21st Century…

PROCEEDINGS of the 22nd International Congress on Acoustics

Isotropy and Diffuseness in Room Acoustics: Paper ICA2016-393

Reproduction of the modal response of enclosures by means of interactive auralization

Diego M. Murillo[a], Filippo M. Fazi[b] and Jeremy Astley[c]

[a]Universidad de San Buenaventura Medellín, Colombia, diego.murillo@usbmed.edu.co
[b]University of Southampton, United Kingdom, Filippo.Fazi@soton.ac.uk
[c]University of Southampton, United Kingdom, rja@isvr.soton.ac.uk

Abstract

A method to create an interactive auralization of the modal response of a room is presented. The process is based on the numerical estimation of the spatial impulse responses of the enclosure using a combination of the finite element method and geometrical acoustics. The acoustic field is then reconstructed by means of a plane wave expansion, which allows for interactive features such as translation of the sound field. The auralization is presented to the listener using a headphone-based binaural system. Compared to techniques based only on geometrical acoustic predictions, this hybrid methodology produces a more accurate rendering of the acoustic field at low frequencies, thus providing an effective tool to reproduce the modal response of enclosures in real-time.

Keywords: Auralization, Plane Wave Expansion, Finite Element Method, Geometrical Acoustics

Reproduction of the modal response of enclosures by means of interactive auralization

1 Introduction

A plane wave expansion of an acoustic field computed by means of the finite element method (FEM) and geometrical acoustics (GA) is proposed as an approach to generate interactive auralizations. The use of FEM improves the estimation at low frequencies yielding a more accurate representation of the modal response of the room. Interactive features such as translation can be straightforwardly implemented in the plane wave domain, which leads to an effective approach to synthesize the modal response of enclosures in real-time.

An acoustic field that satisfies the homogeneous Helmholtz equation can be represented by means of a plane wave expansion as

$$p(\mathbf{x},\omega) = \int_{\widehat{\mathbf{y}}\in\Omega} e^{jk\mathbf{x}\cdot\widehat{\mathbf{y}}} q(\widehat{\mathbf{y}},\omega) d\Omega(\widehat{\mathbf{y}}), \tag{1}$$

in which $\mathbf{x}$ is the evaluation point, $\widehat{\mathbf{y}}$ indicates the different incoming directions of the plane waves density, $q(\widehat{\mathbf{y}},\omega)$ is the amplitude density function and Ω is the unitary sphere. For the implementation of the method, equation 1 must be discretized into a finite number of L plane waves, namely

$$p(\mathbf{x},\omega) = \sum_{l=1}^{L} e^{jk\mathbf{x}\cdot\widehat{\mathbf{y}}_l} q_l(\omega)\Delta\Omega_l, \tag{2}$$

where $\Delta\Omega_l$ corresponds to the portion of the unit sphere that is associated by the plane wave l. The discretization of equation (1) can be performed using a predefined uniform distribution of L plane waves over a unit sphere [1]. Nevertheless, the use of a finite number of plane waves determines a reduction of the area in which the sound field synthesis is accurate. Kennedy et al. [2] proposed the following relation between the area of accurate reconstruction, the number of plane waves and the frequency of the field

$$L = \left(\left\lceil e\pi\frac{R}{\lambda}\right\rceil + 1\right)^2, \tag{3}$$

in which L is the number of plane waves, $\lceil\cdot\rceil$ indicates the round operator, e is Euler's number, λ is the wavelength and R is the radius of a sphere within which the reconstruction is accurate.

1.1 Translation of acoustic fields based on a plane wave expansion

Figure 1 illustrates the vector $\mathbf{x}'$, which identifies the origin of a relative coordinate system corresponding to the center of the listener's head, such that the relative vector $\mathbf{x}_{\text{rel}}$ correponds the same point in space as that identified by the vector $\mathbf{x}$ in absolute coordinates. Therefore $\mathbf{x}_{\text{rel}} = \mathbf{x} - \mathbf{x}^{'}$.

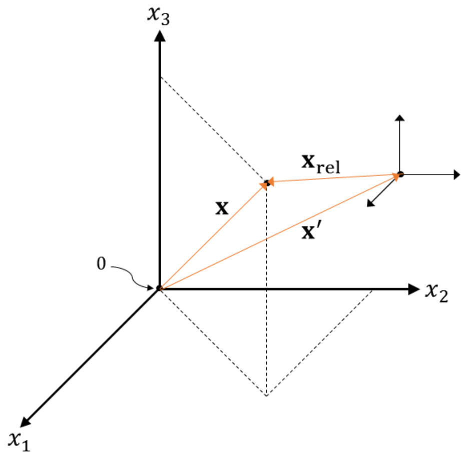

Figure 1: vector $\mathbf{x}$ is represented as $\mathbf{x}_{\text{rel}}$ in the relative coordinate system $\mathbf{x}^{'}$

The sound field translation operator is derived from considering two plane wave expansions of the same sound field but centered at different points in space, specifically, at the origin of the absolute and relative coordinate systems. In this case, the difference between the two plane wave expansions is given by the plane wave amplitude densities $q(\hat{\mathbf{y}}, \omega)$ and $q_{\text{rel}}(\hat{\mathbf{y}}, \omega)$, respectively. The plane wave expansion of the sound field p centered at the origin of the absolute coordinate system is defined as

$$p(\mathbf{x}, \omega) = \int_{\hat{\mathbf{y}} \in \Omega} e^{jk\mathbf{x}\cdot\hat{\mathbf{y}}} q(\hat{\mathbf{y}}, \omega) d\Omega(\hat{\mathbf{y}}), \tag{4}$$

where Ω is the unitary sphere. Similarly, the plane wave expansion of the same filed p but centered at the origin of the relative coordinate system is expressed as

$$p(\mathbf{x}, \omega) = \int_{\hat{\mathbf{y}} \in \Omega} e^{jk\mathbf{x}_{\text{rel}}\cdot\hat{\mathbf{y}}} q_{\text{rel}}(\hat{\mathbf{y}}, \omega) d\Omega(\hat{\mathbf{y}}). \tag{5}$$

It is important to to point out that the plane wave densities $q(\hat{\mathbf{y}}, \omega)$ and $q_{\text{rel}}(\hat{\mathbf{y}}, \omega)$ are different functions. Therefore, the objective is to express one density in terms of the other. This is achieved by expanding $\mathbf{x}_{\text{rel}}$ as $\mathbf{x} - \mathbf{x}^{'}$, namely

$$p(\mathbf{x}, \omega) = \int_{\hat{\mathbf{y}} \in \Omega} e^{jk\mathbf{x}\cdot\hat{\mathbf{y}}} e^{-jk\mathbf{x}^{'}\cdot\hat{\mathbf{y}}} q_{\text{rel}}(\hat{\mathbf{y}}, \omega) d\Omega(\hat{\mathbf{y}}). \tag{6}$$

The two representations of $p(\mathbf{x}, \omega)$ given by equations (4) and (6) are equivalent expansions of the same field. Equating these two equations yields

$$\int_{\widehat{\mathbf{y}}\in\Omega} e^{jk\mathbf{x}\cdot\widehat{\mathbf{y}}} q(\widehat{\mathbf{y}},\omega) d\Omega(\widehat{\mathbf{y}}) = \int_{\widehat{\mathbf{y}}\in\Omega} e^{jk\mathbf{x}\cdot\widehat{\mathbf{y}}} e^{-jk\mathbf{x}'\cdot\widehat{\mathbf{y}}} q_{\text{rel}}(\widehat{\mathbf{y}},\omega) d\Omega(\widehat{\mathbf{y}}), \tag{7}$$

whose solution for $q_{\text{rel}}(\hat{\mathbf{y}},\omega)$ is given by

$$q_{\text{rel}}(\widehat{\mathbf{y}},\omega) = q(\widehat{\mathbf{y}},\omega) e^{jk\mathbf{x}'\cdot\widehat{\mathbf{y}}}. \tag{8}$$

Equation (8) indicates that the plane wave density $q_{\text{rel}}(\widehat{\mathbf{y}},\omega)$ can be predicted by taking the product between the plane wave density function of the plane wave expansion centered at the origin $q(\widehat{\mathbf{y}},\omega)$ and a complex exponential whose argument depends on the vector $\mathbf{x}'$. In other words, $e^{jk\mathbf{x}'\cdot\widehat{\mathbf{y}}}$ is the translation operator for the plane wave expansion from the origin to $\mathbf{x}'$. Its equivalence in the time domain can be easily found by using the shifting property of the Fourier transform [3]

$$\int_{-\infty}^{\infty} F(t-t') e^{-j\omega t} = f(\omega) e^{-j\omega t'}. \tag{9}$$

Equation 9 indicates that the product between a complex function $f(\omega)$ and a complex exponential is equivalent to shifting the function $F(t)$ according to the argument of the complex exponential. This means that the translation operator basically corresponds to the application of delays in the time domain, namely

$$Q_{\text{rel}}(\widehat{\mathbf{y}},t) = Q\left(\widehat{\mathbf{y}}, t - \frac{\mathbf{x}'\cdot\widehat{\mathbf{y}}}{c}\right). \tag{10}$$

2 Methods

Different strategies are proposed to generate a plane wave representation from the FE and GA simulations. In the case of FEM, an implementation of an inverse method is proposed to calculate the complex amplitudes $q(\omega)$ of a set of L plane waves that reconstruct a selected target acoustic field. For geometrical acoustics, the reflections that contribute to the omnidirectional room impulse response predicted at the origin where the plane wave expansion is performed are traced using a virtual high-directional resolution microphone [6]. The plane wave expansion is generated by assuming that the reflection paths are in fact plane waves propagating inside of the enclosure.

2.1 Plane wave expansion from finite element simulations

The acoustic pressure estimated from FEM at a specific location of the domain can be understood as the output from an omnidirectional microphone. The combination of different acoustic pressure points generates a virtual microphone array which can be used to extract spatial information of the sound field. Based on that information, the amplitude $q(\omega)$ of each plane wave is determined by the inversion of the transfer function matrix between microphones and plane waves [4]. The complex acoustic pressure at *M* virtual microphone positions is denoted using vector notation as

$$\mathbf{p}(\omega) = [p_1(\omega), p_m(\omega), \dots, p_M(\omega)]^T, \quad (11)$$

where p_m is the acoustic pressure at the m-th virtual microphone. Likewise, the complex amplitudes of L plane waves used to reconstruct the sound field are represented by the vector

$$\mathbf{q}(\omega) = [q_1(\omega), q_l(\omega), \dots, q_L(\omega)]^T. \quad (12)$$

Finally, the transfer function that describes the sound propagation from each plane wave to each virtual microphone can be arranged in matrix notation as:

$$\mathbf{H}(\omega) = \begin{vmatrix} h_{11}(\omega) & \cdots & h_{1L}(\omega) \\ \vdots & h_{ml}(\omega) & \vdots \\ h_{M1}(\omega) & \cdots & h_{ML}(\omega) \end{vmatrix}$$

in which $h_{ml} = e^{jk\mathbf{x}_m \cdot \hat{\mathbf{y}}_l}$. Consequently, the relationship between the plane wave amplitudes and the virtual microphone signals is

$$\mathbf{p}(\omega) = \mathbf{H}(\omega)\mathbf{q}(\omega). \quad (13)$$

The amplitude of the plane waves is calculated solving equation (13) for $\mathbf{q}(\omega)$. This is carried out in terms of a least squares solution, which minimizes the sum of the squared errors between the reconstructed and the target sound field [4]. In the case of an overdetermined problem (more virtual microphones than plane waves), the error vector can be expressed as

$$\mathbf{e}(\omega) = \mathbf{p_r}(\omega) - \mathbf{p_t}(\omega), \quad (14)$$

where $\mathbf{p_r}(\omega)$ is the reconstructed pressure by the plane wave expansion and $\mathbf{p_t}(\omega)$ is the target pressure from the FEM model. The least squares solution is achieved by the minimization of a cost function $J(\omega) = \mathbf{e}^H(\omega)\mathbf{e}(\omega)$ in which $(\cdot)^H$ indicates the Hermitian transpose. The minimization of the cost function $J(\omega)$ is given by [4]

$$\mathbf{q}(\omega) = \mathbf{H}^\dagger(\omega)\mathbf{p}(\omega), \quad (15)$$

in which $\mathbf{H}^\dagger(\omega)$ is the Moore-Penrose pseudoinverse of the propagation matrix $\mathbf{H}(\omega)$ [4].

A hypothetical rectangular enclosure of dimensions 5m, 10m and 3m with origin at the left-bottom corner of the room has been considered as a reference case for the simulations. A FE model was created using the commercial package Comsol V4.4 to predict the frequency response due to a monopole source located at (4.5, 9.5, 1.5). The boundary conditions were characterized using a uniform resistive specific acoustic impedance value over all the boundaries of the domain. The value was selected to obtain a diffuse absorption coefficient of 0.15. The relation which has been assumed between the specific acoustic impedance and the diffuse absorption coefficient α_d is [5]

$$\alpha_d = 8\Gamma\{1-\Gamma\ln\left[\frac{r_n}{\Gamma}+2r_n+1\right]+\left(\frac{x_n}{r_n}\right)\Gamma\left(\left(\frac{r_n}{x_n}\right)^2-1\right)\tan^{-1}\left(\frac{x_n}{(r_n+1)}\right)\}, \tag{16}$$

in which r_n and x_n are the real and imaginary part, respectively, of the specific acoustic impedance Z_n non-dimensionalized by $\rho_0 c$, and $\Gamma = r_n/(r_n^2+x_n^2)$. By setting the imaginary part of the acoustic impedance to zero it is possible to calculate a resistive part which can be used in FE simulations. For a specific value of α_d, r_n is given by the solution of

$$\alpha_d = \frac{8}{r_n}\left\{1-\frac{1}{r_n}\ln\left(1+2r_n+r_n^2\right)+\frac{1}{1+r_n}\right\}. \tag{17}$$

A configuration of 64 plane waves and a cube-shape microphone array with linear dimensions of 1.6 m (spatial resolution of 0.2 m) was selected for the implementation inverse method. Figure 2 shows the real part of the target (a) and the reconstructed (b) acoustic pressure in Pa at 63 Hz in a cross-section of the domain (z = 1.5m). Part (c) of the figure corresponds to a normalized error, which is defined as

$$E_n(\mathbf{x},\omega) = 10\log_{10}\left(\frac{|p(\mathbf{x},\omega)-\tilde{p}(\mathbf{x},\omega)|^2}{|p_t(\mathbf{x},\omega)|^2}\right). \tag{18}$$

where $\tilde{p}(\mathbf{x},\omega)$ is the reconstructed pressure and $p(\mathbf{x},\omega)$ is the target pressure. The black squared presented in Figure 2 represents the position of the microphone array, the white contour defines the region within which the normalized error is smaller than -20 dB and the black circle corresponds to the area of accurate reconstruction predicted by equation (3).

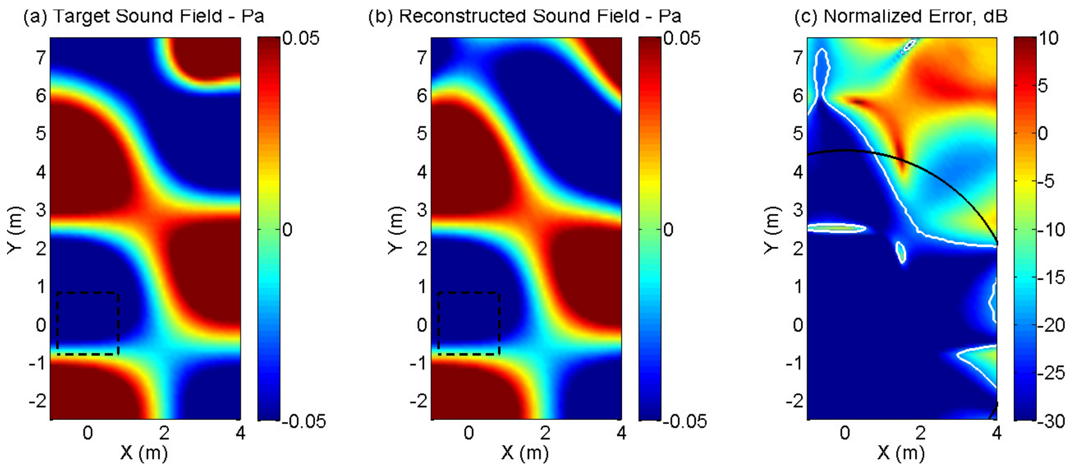

Figure 2: Target and reconstructed field at 63 Hz

Figure 2 indicates that the inverse method is a suitable approach to estimate the complex amplitudes of a plane wave expansion that synthesizes an acoustic field, which has been predicted by the finite element method. A good agreement was found between the area of accurate reconstruction predicted by equation (3) and the region where the normalized error is below -20 dB.

2.2 Plane wave expansion from geometrical acoustic simulations

Simulations were conducted using the commercial package Catt-Acoustics V9. The boundary conditions were characterized with a uniform diffuse absorption and scattering coefficients of 0.15 and 0.1, respectively. Then, an external tool developed by Catt-Acoustic was implemented to extract directional information of the acoustic field. RerflPhinder v.1.0c is a software that allows directional impulse responses to be created using a patented high-resolution virtual microphone (*sector mic*) [6]. The algorithm creates a virtual microphone with a given directivity pattern covering a square window whose aperture can be selected according to different resolutions. The output of the *sector mic* corresponds to a directional impulse response composed only by the contributions of the reflections whose direction agree with the directivity pattern. An angle of 10 degrees was used to sample the unit sphere yielding to a 614 directional impulse responses.

Figure 3 shows the frequency response and the energy distribution based on a 1/3 octave band resolution of the sum of the directional impulse responses and the mono impulse response predicted at the central point of the expansion.

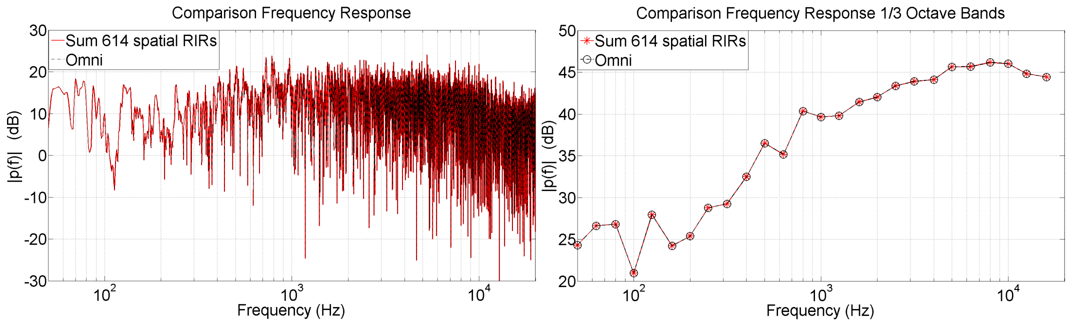

Figure 3: Comparison of room frequency responses (mono and sum of directionals)

One important assumption made for the encoding of directional information from GA simulations is the consideration of plane waves as the only type of wave that contributes to the directional impulse responses. This assumption is reasonable for far field propagation; equation (19) establishes the relation between distance and frequency where far field can be considered.

$$kr \gg 1, \tag{19}$$

where k is the wavenumber and r is the distance from the receiver to the acoustic source. The direct path between the source and the receiver is approximately 8.6 m leading to a frequency of 63 Hz considering at least one order of magnitude. The GA data is used from 355 Hz, which is high enough to assume a plane wave propagation for this specific case.

The spatial information extracted from GA simulations corresponds to 614 directional impulse responses. This information has to be transformed in order to generate a common ground with the plane wave expansion from the FE data. This means the directional impulse responses must be modified according to the $L = 64$ possible directions given by the plane wave locations selected to recreate the sound field in the case of FEM. A spherical harmonic interpolation was adopted for this purpose. The Jacobi-Anger expansion allows to describe a plane wave in terms of spherical harmonics [3]. Based on that, each reflection is encoded using a 7th order. Subsequently, the complex spherical harmonic coefficients are decoded into a finite set of plane waves following a mode-matching approach. The directions of the plane waves correspond to the 64 directions used to process the FE data.

$$4\pi \sum_{n=0}^{N=7} j^n j_n(kr_x) \sum_{m=-n}^{n} Y_n^m(\theta_x,\phi_x) Y_n^m(\theta_y,\phi_y)^* = 4\pi \sum_{l=1}^{L} q_l \sum_{n=0}^{N=7} j^n j_n(kr_x) \sum_{m=-n}^{n} Y_n^m(\theta_x,\phi_x) Y_n^m(\theta_l,\phi_l)^*, \tag{20}$$

The simplification of equation 20 using the orthogonality relation of the spherical harmonics yields to the following mode-matching equation for each n and m

$$Y_n^m(\theta_y,\phi_y)^* = \sum_{l=1}^{L} q_l Y_n^m(\theta_l,\phi_l)^*, \tag{21}$$

for $n = 0 \ldots N$ and $|m| \leq n$. This finite set of linear equation are solved in terms of the least squared solution by applying an inverse method. The formulation for the 614 plane waves corresponds to

$$\tilde{\mathbf{q}} = \mathbf{C}^{\dagger}\mathbf{A}\mathbf{q}, \tag{22}$$

in which

$$\mathbf{C} = \begin{vmatrix} Y_{00}(\theta_1,\phi_1)^* & \cdots & Y_{00}(\theta_L,\phi_L)^* \\ \vdots & Y_{nn}(\theta_l,\phi_l)^* & \vdots \\ Y_{NN}(\theta_1,\phi_1)^* & \cdots & Y_{NN}(\theta_L,\phi_L)^* \end{vmatrix}$$

$\mathbf{A} = [\mathbf{a}_1 \cdots \mathbf{a}_i]$, $\mathbf{a}_i = \left[Y_0^0(\theta_i,\phi_i)^* \cdots Y_N^N(\theta_i,\phi_i)^*\right]^T$, $i = 614$, $\mathbf{q} = [q_1 \cdots q_i]^T$ and $\tilde{\mathbf{q}} = [q_1 \cdots q_L]^T$.

2.3 Combination of the FE and GA data

The combination of the plane wave expansions is carried out in the frequency domain by applying 8th order Butterworth filters. Each element of the PWE computed from the FE data is filtered using a low-pass filter. In accordance, the directional impulse responses of the PWE from GA are transformed to the frequency domain by applying a Fourier transform. Then, the signals are filtered using a high-pass filter. The crossover frequency for the filters was 355 Hz, which is the central frequency of the 1/3 octave band previous to the maximum frequency simulated in FEM. This ensures that the FE data is not abruptly truncated.

The unified directional impulse responses are computed by adding the filtered plane wave expansions and by applying an inverse Fourier transform. The final outcome corresponds to $L = 64$ directional impulse responses, which can be processed to generate interactive auralizations.

2.4 Implementation

An implementation was carried out using the commercial packages Max v.7.2 and Unity v.5.0. Max is used as the audio rendering engine whilst Unity has been adopted to generate a platform in which the listener can move using a first-person avatar and listen to the changes in the acoustic field based on its position in the enclosure. The interaction between these two software packages was achieved using the Max-Unity Interoperability Toolkit [7]. The auralization are reproduced using a headphone-based binaural system, which convolves the directional impulse responses with the HRTFs corresponding to their incoming directions. Figures 4 illustrates the model developed in Unity to generate the interactive auralization.

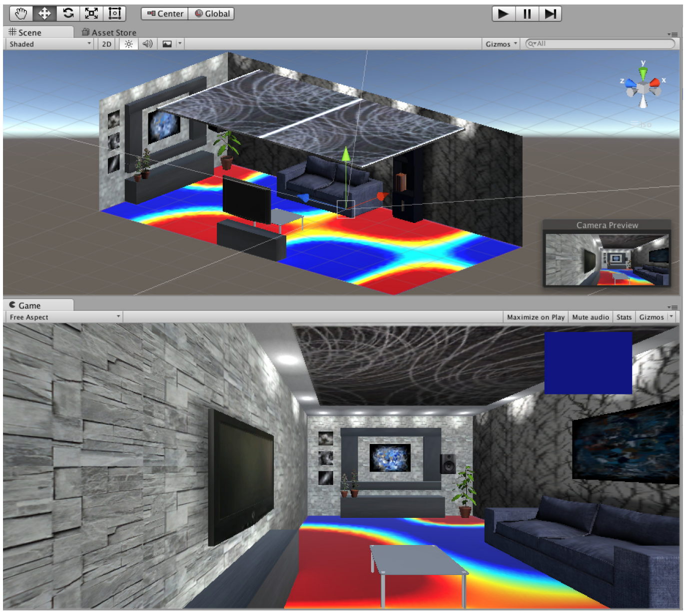

Figure 4: Rectangular room created in Unity

3 Results

A comparison of the predicted omnidirectional frequency responses at different receiver positions is considered for different enclosures. This is performed by rendering the sound field in real-time using an auralization system developed in Max whose directional impulse responses were estimated based on FE and GA simulations as described above. The omnidirectional frequency responses from the interactive auralization system were obtained by summing all the directional impulse responses and recording the total output. This information is compared to omnidirectional frequency responses that were synthesized individually at the receiver locations using a combination of the finite element method and geometrical acoustics. These omnidirectional references do not use the plane wave expansion information, They correspond to the frequency response of omnidirectional receivers obtained directly from the commercial packages Comsol and Catt-Acoustics, respectively.

Figure 5 illustrates the position of 4 receivers which have been selected for the analysis. A0 identifies the source position and 01 corresponds to the central point of the expansion. Figures 6 to 9 show the frequency response and the 1/3 octave band energy distribution for each receiver position. The cyan vertical line indicates the crossover frequency (355 Hz) and the black line indicates the predicted maximum frequency in which the translation should be correctly performed. The maximum frequency was estimated solving equation (3) for R. Furthermore, due to the stochastic implementation of the scattering coefficients in the GA simulations, an exact reconstruction is only achieved at the central point of the expansion. Beyond that, only an agreement with the omnidirectional references is expected only in terms of energy at high frequencies.

The mean error displayed in the figures was selected as a metric and it is defined as:

$$\mathrm{ME(dB)} = \frac{1}{n}\sum_{i=1}^{n}\left|10\log_{10}(|\widetilde{p}_i|^2) - 10\log_{10}(|p_i|^2)\right|, \tag{23}$$

in which n is the number of 1/3 octave frequency bands, $|\widetilde{p}_i|^2$ and $|p_i|^2$ are the predicted and reference energy of the acoustic presure in the i-th 1/3 octave band, respectively. This error considers an equal contribution of all the frequency bands, thus being similar to a model in which pink noise have been used as input signal. This metric was selected to provide an insight of how dissimilar is in average the reconstructed signal with respect to the reference one.

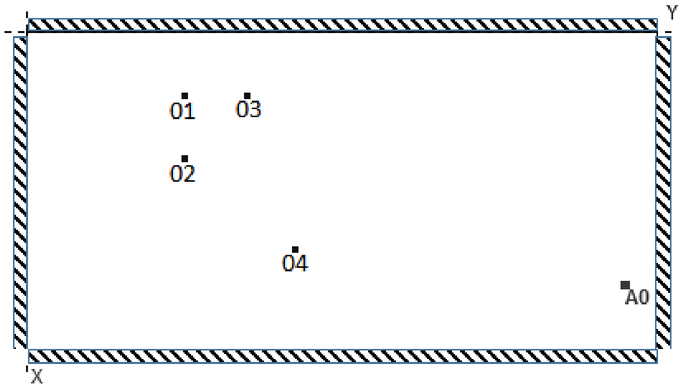

Figure 5: Sketch of the rectangular room, receiver positions

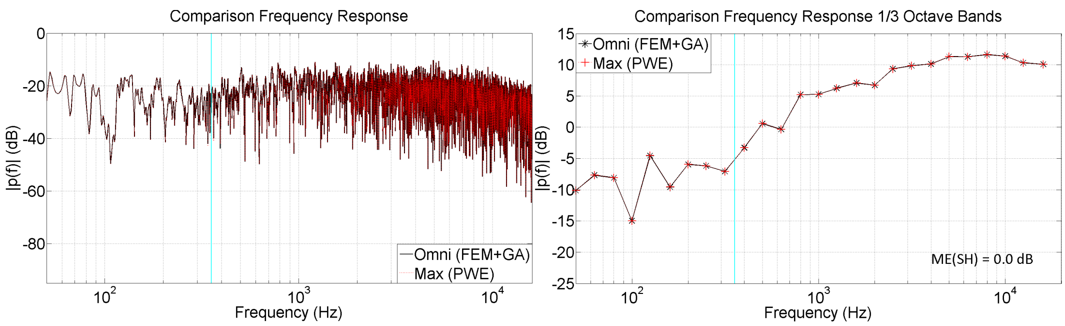

Figure 6: Comparison of frequency responses. PWE (FEM+GA) and omnidirectional RIR (FEM+GA) at the reference position 1

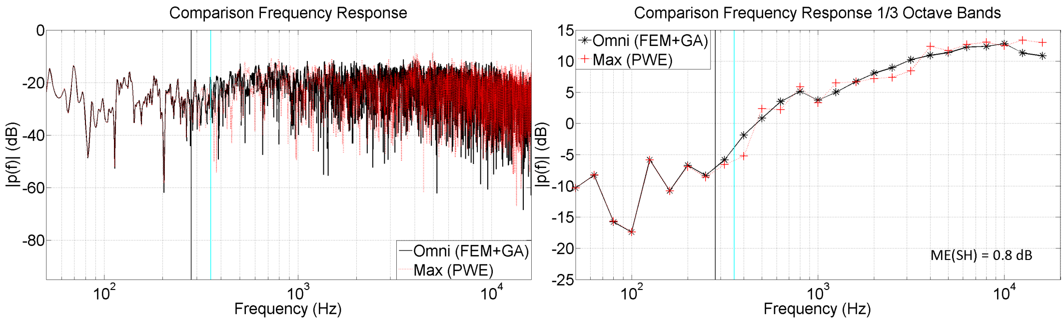

Figure 7: Comparison of frequency responses. Translated PWE (FEM+GA) and omnidirectional RIR (FEM+GA) at the translated position 2. 1 m from the central point of the expansion

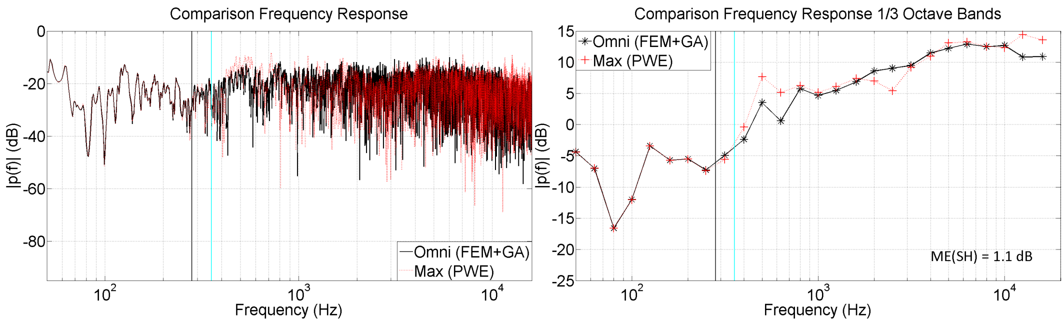

Figure 8: Comparison of frequency responses. Translated PWE (FEM+GA) and omnidirectional RIR (FEM+GA) at the translated position 3. 1 m from the central point of the expansion

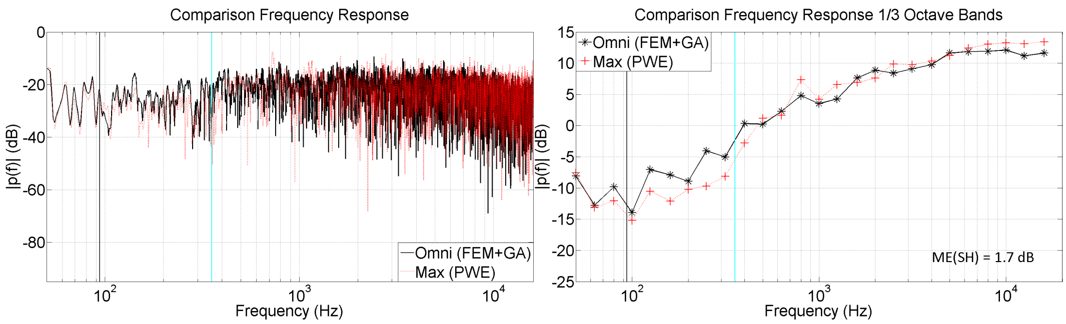

Figure 9: Comparison of frequency responses. Translated PWE (FEM+GA) and omnidirectional RIR (FEM+GA) at the translated position 4. 3 m from the central point of the expansion

The results indicate an excellent agreement to the reference data below the frequency predicted by equation (3). Smaller differences found in this frequency range may be associated to two reasons: the implementation of integer delays in Max and the numerical accuracy used by

Max to perform mathematical operations (summing the directional impulse responses). Above the crossover frequency, a good agreement in terms of energy was achieved for all the receivers. A significant mismatch was found in the frequency range between 160 Hz and 315 Hz at the receiver's position 4. This outcome is related to the situation where the frequency predicted by equation (3) is much lower than the crossover frequency. In this case, the translation operator was applied to predict the acoustic field at a distance which is much larger than the radius of the maximum region of accurate sound field reconstruction.

4 Conclusions

A methodology to reproduce the modal response of an enclosure in real-time has been presented. The approach is based on a plane wave representation of an acoustic field, which has been predicted by means of the finite element method and geometrical acoustics. This acoustic representation not only allows for interactive features such as the translation of the sound field, but also is compatible with a several sound reproduction techniques such as binaural, Ambsonics, WFS and VBAP. The use of FEM leads to an improvement in the acoustic prediction at low frequencies, thus making the proposed approach ideal for the evaluation of the modal response of enclosures.

A real-time implementation has been presented, which allows the listener to move around to a virtual enclosure and listen the changes in the acoustic field. This is done by the application of a translation operator in the plane wave domain. An analytical expression for the translation of plane waves has been presented.

The results indicate that the proposed methodology is able to reconstruct with good accuracy the acoustic field in real-time. However, the discretization of the plane wave expansion leads to a shrink in the area where the reconstruction is accurate yielding a local description of the sound field.

References

[1] Fliege, J. Sampled Sphere. Technical report, University of Dortmund, Dortmund, 1999.

[2] Kennedy, R., Sadeghi, P. Abhayapala, T. and Jones, H. Intrinsic Limits of Dimensionality and Richness in Random Multipath Fields, IEEE Transactions on Signal Processing, 55(6):2542–2556, 2007.

[3] Williams, E. Fourier Acoustics. Academic Press, London, 1st edition, 1999.

[4] Nelson, P. and Yoon, S. Estimation of Acoustic Source Strength By Inverse Methods: Part I, Conditioning of the Inverse Problem, Journal of Sound and Vibration, 233(4):639–664, 2000.

[5] Fahy, F. Foundations of Engineering Acoustics. Academic Press, Oxford, 1st edition, 2008.

[6] Dalenback, B. Syntes av virtuell direktiv mikrofon, Patent SE 534861 C2, 2012.

[7] Department of Music. Virginia Tech-School of Performing Arts, 2015. URL http://disis.music.vt.edu/main/index.php.